IMPORTANCE OF ADDING PERTURBATIONS IN THE OPTIMIZED BOUNDARY VALUE INITIAL ORBIT DETERMINATION USING SHOOTING METHOD

H.K. Mann, A. Vananti, and T. Schildknecht

Astronomical Institute of University of Bern, 3012 Bern, Switzerland, Email: {harleen-kaur.mann, alessandro.vananti, thomas.schildknecht}@aiub.unibe.ch

ABSTRACT

Space debris is becoming a major threat for functional spacecraft. Since, out of thousands of tracked objects in the Earth's orbits, only a small percentage corresponds to the operational satellites. It is clear that this problem needs to be addressed immediately. The first step towards solving it requires the monitoring of the space environment and cataloguing the debris. This work focuses on the high-altitude orbits (near GEO regime) which is done using optical surveys. The latter result in angles-only observations of objects on very short arcs when compared to the periods of these orbits. These observations are sparse and cover a very small part of the orbit, hence the initial orbit determination becomes challenging. Two observation series are associated together to find out if they belong to the same object and an initial orbit is computed. One way to do it is by using the Optimized Boundary Value Initial Orbit Determination (OBVIOD). This algorithm does not include perturbations. To include the latter we use a so-called shooting method. The shooting scheme is a boundary-value approach, which works like an initial-value method. It takes a hypothesis at the initial boundary and propagates it to the second boundary, where the computed value and the original boundary value are compared. The hypothesis, which gives the desired output at the second boundary, is accepted as the solution. In the proposed algorithm, the propagation from the initial boundary to the final one involves perturbations such as solar radiation pressure, Earth's geopotential terms, solar and lunar gravitational forces. A root finding method based on bisection is used inside the shooting method. An admissible region originating from the semi-major axis is used in order to reduce the number of scenarios to be computed. In the original version of the OBVIOD, the initial orbit determination takes place by solving the Lambert's problem. This version does not work well for the high area-to-mass (AMR) objects, especially over multiple revolutions. In this paper, OBVIOD's performance is compared with the new shooting OBVIOD for different AMR values and varied number of revolutions between the boundaries. This comparison helps to identify the cases where it becomes important to make use of the proposed algorithm.

Keywords: OBVIOD; IOD; AMR; perturbations.

1. INTRODUCTION

Space debris are defined as non- functional, man-made objects in space with no reasonable expectation of assuming or resuming its intended function [2]. It is essential to observe and catalogue them in order to avoid collisions with the active satellites. Optical surveys are conducted to observe the objects in the geostationary region. These surveys yield short sequences of angle measurements, called tracklets, which cover a small fraction of the overall orbit [3]. [4] proposed an orbit determination method using available information of two tracklets. This approach works with a boundary-value formulation and uses an optimization scheme to find the best fitting orbits (OBVIOD). It solves the Lambert problem, a special case of the orbital boundary value problem, which consists of two position vectors at separate epochs. The Initial Orbit Determination (IOD) in OBVIOD provides an unperturbed solution.

In order to add perturbations in the IOD, a so-called shooting method is proposed here. Following sections will show the working of the latter.

1.1. Working in OBVIOD

[4] introduced a method where an optimization scheme is used to identify tracklets of common objects. The angle measurements consist of series of α (right ascension) and δ (declination) values. Linear regression is performed over these series, resulting in average α, δ values and the corresponding $\dot{\alpha}$, $\dot{\delta}$ for a meantime. This set of values is called the attributable vector [9]. Using the attributable vectors over simple measurements provides an advantage as the angular rates information is now available. Moreover, the mean angular positions, rates obtained from the linear regression will have higher accuracy compared to the raw observations. The next step involves a range hypothesis, which is used with the line of sight vectors and station positions to compute position vectors. The Lambert's problem is solved, giving velocities at both epochs.

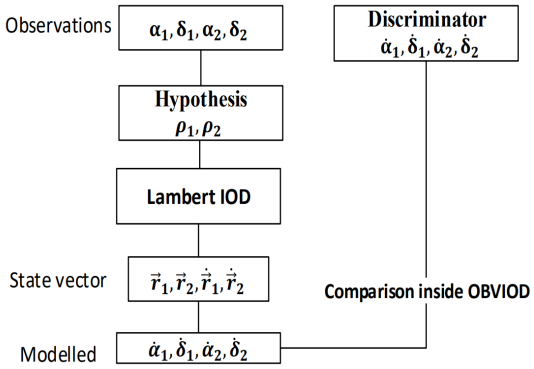

Figure 1. Process Flow in OBVIOD.

The angular rates obtained from the previous step are compared with the ones from the attributable vector using a loss function. The latter is based on the difference between the measured and the modeled angular rates scaled by the uncertainty. In this case, the Mahalanobis distance is used as the loss function. For a distribution y, with mean $\overline{y}$ and covariance matrix C_y , the Mahalanobis distance for each point y_i is defined by [6]:

$$D_M(y) = \sqrt{(y_i - \overline{y})^T C_y (y_i - \overline{y})} \tag{1}$$

A minimization algorithm called Broyden Fletcher Goldfarb Shanno (BFGS) is used to search for the loss function minimum. [5] briefly explain the working of this algorithm. If the Mahalanobis distance is below a certain threshold, the tracklets are said to be correlated. In other words, they are assumed to belong to the same object. The range hypothesis corresponding to the minimum is accepted and the initial orbit is computed for these tracklets. Figure 1. shows the schematic of OBVIOD.

1.2. Limitations due to use of unperturbed Lambert solution

The IOD inside OBVIOD takes place by solving the Lambert orbit determination problem using the method from [7]. The Lambert's initial orbit determination algorithm mentioned in [7] uses the Lambert problem's geometry to derive new variables in order to solve the problem. The derivations originate from the expression of time of flight (t_f) as shown in equation (2).

$$\sqrt{\mu} t_f = a^{\frac{3}{2}} [2N\pi + \alpha - \beta - (\sin\alpha - \sin\beta)] \tag{2}$$

Here $\mu = GM_{earth}$, N is the number of revolutions covered by the object, a is the semi major axis of the orbit, and t_f is the time taken to reach from the first position to the second position. α and β are defined as follows:

$$sin(\frac{\alpha}{2}) = [\frac{s}{2a}]^{\frac{1}{2}} \tag{3}$$

$$sin(\frac{\beta}{2}) = [\frac{(s-c)}{2a}]^{\frac{1}{2}} \tag{4}$$

Where $s = (r_1 + r_2 + c)/2$, r_1 and r_2 are geocentric positions at the first and second epoch. c is the length of the chord connecting position at first epoch and position at second epoch. An important parameter used to solve the Lambert's problem in this algorithm is λ, which is defined as:

$$\lambda^2 = \frac{(s-c)}{s} \tag{5}$$

This algorithm assumes no perturbations while solving the initial orbit determination problem. There are some scenarios where this algorithm begins to fails or becomes inaccurate. Some of the problems faced are described below:

1. Ambiguity near full revolutions: The line of sight vectors at the first epoch $\overrightarrow{u_1}$ and second epoch $\overrightarrow{u_2}$ almost overlap each other near full revolutions. The angle between $\overrightarrow{u_1}$ and $\overrightarrow{u_2}$ is called the transfer angle, it approaches zero if a full revolution case is concerned. This leads to the ambiguity of no. of revolutions and also the solution to be used [7], [8]. Hence, the solution provided by the Lambert algorithm in these cases is not reliable.

2. Time of flight (tof) not computed for highly perturbed orbits: The algorithm proposed by Izzo [7] involves various steps. A variable called x is defined, which is to be used as the iteration variable. It can be expressed as:

$$x = cos\frac{\alpha}{2} \tag{6}$$

or,

$$x = cosh\frac{\alpha}{2} \tag{7}$$

where α is the angle derived from Lambert problem's geometry and given in equation (2). The Lambert solver iterates on the Lancaster-Blanchard variable x using a Householder iteration scheme. Following this, various other variables are defined using x, λ. Finally the non-dimensional time of flight equation is derived, which is valid in all cases (parabolic, hyperbolic and elliptic). The time-of-flight expression defined in the algorithm is also not valid for cases where $x = 0$ and $x = 1$. The derivations assume a non - perturbed motion of the object. The value of x is provided by initial guesses found exploiting the curve shape in a $\tau - \epsilon$ plane. τ and ϵ are defined in terms of x and T (non-dimensional time of flight) respectively.

Once the initial value of x is supplied, the Householder iterations take place. A new value of non-dimensional tof and x is computed in every iteration and until the error is below tolerance, the iterations continue. The error term is defined as:

$$err = abs(x_0 - x_{new}) \tag{8}$$

The value of tof is computed using either Lagrange, Battin or Lancaster formula [7] depending on the value of x. Figure 2. shows a case where the iterations take place using Lancaster formula. The tof equation in this case is as follows:

$$tof = \frac{(x - \lambda z - \frac{d}{y})}{E} \tag{9}$$

where d, z, y and E are defined as

$$\begin{aligned} E &= x^2 - 1; \\ K &= \lambda^2; \\ z &= \sqrt{1 + KE}; \\ y &= \sqrt{abs(E)}; \\ d &= log(f + g); \\ f &= y(z - \lambda x); \\ g &= xz - \lambda E; \end{aligned} \tag{10}$$

The screenshot in Figure 2. shows that $(f + g) < 0$, which makes $d = NaN$. This subsequently leads towards the failure to compute a value of tof. The values of velocity are not computed and one does not get a solution for the initial orbit. Since this Lambert algorithm assumes an unperturbed geometry, it gives wrong / unexpected values of the variables which makes the algorithm fail in some cases.

3. Divergence due to Lambert solution being far from perturbed solution: If a full failure does not occur as shown in the previous case, there will still be some differences from the real solution because of the presence of perturbations. The difference between the Lambert solution and the real solution mainly depends on the time of flight (number of revolutions) between the two tracklets and the AMR value.

2. SHOOTING METHOD

The shooting method belongs to the class of two-point boundary value problems. It treats the boundary value problem as an initial value problem. It chooses an initial value of the dependent variable at the first boundary, propagates the function to arrive at the other boundary. This solution is compared with the second boundary value. Free parameters at the first boundary are adjusted to satisfy the desired second boundary value. Figure 3. shows how the different initial values of the dependent variable are taken at the first boundary value in order to reach the desired boundary value [5].

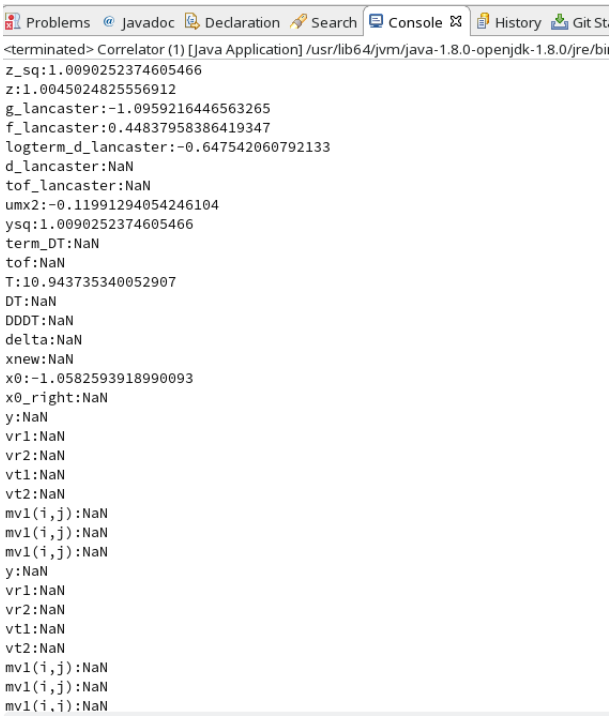

Figure 2. An example showing a case when the lambert algorithm fails for a highly perturbed orbit.

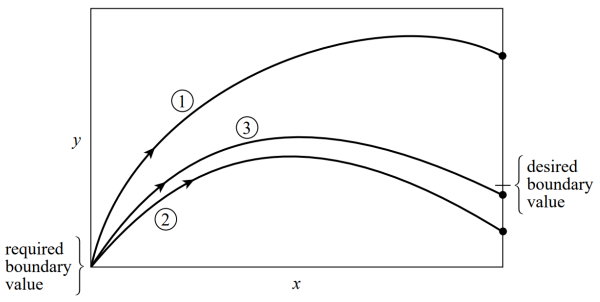

Figure 3. Working of shooting method.

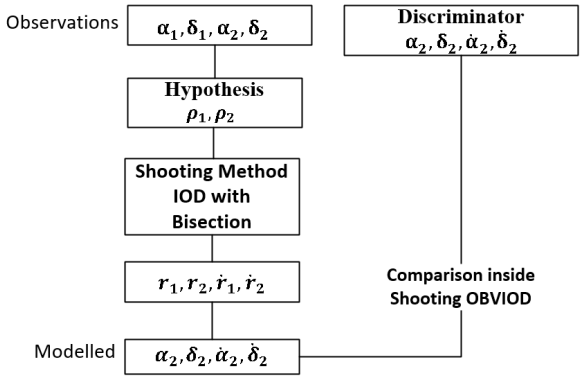

Figure 4. Process Flow in Shooting-OBVIOD.

2.1. Shooting method in OBVIOD

The boundary values in the case of Shooting-OBVIOD are angular measurements at both the epochs. Using the attributable vector one has the mean angular positions and rates. The range hypothesis is made for both the boundaries. The station position and velocity at both the epochs is known, the only unknown parameter at the initial epoch is $\dot{\rho_1}$ (range-rate). It is chosen as the free parameter inside Shooting IOD and is hypothesized at the initial epoch. The orbit is computed at this epoch and propagated to the second epoch. The propagation step involves perturbations such as solar radiation pressure, Earth's geopotential terms, solar and lunar gravitational forces.

The second boundary value inside shooting IOD is ρ_2 (range at second epoch). The ρ_{2j} obtained during the shooting method iterations is compared with the ρ_2 hypothesis made in OBVIOD iterations before entering shooting. The iteration parameters inside Shooting-OBVIOD remain to be ρ_1 (range at first epoch) and ρ_2. This is based on the analysis done by [4] on the loss functions and performance. The change of variables from (ρ_1, ρ_2) to $(\dot{\rho_1}, \rho_1)$ takes place inside shooting in order to allow for a propagation from the initial epoch to the final epoch for the pair ρ_1, ρ_2. This is because the shooting method allows for IOD for the given pair with the addition of perturbations.

The method is described more in detail in the following sections. The Shooting IOD replaces the Lambert IOD during the minimization of the loss function. The resulting schematic of Shooting-OBVIOD is shown in Figure 4.

2.2. Bisection method in shooting

A root finding algorithm is needed which is reliable in terms of convergence. An analysis is done in [1] and the bisection method is chosen to be used inside the Shooting IOD. It works by searching for the point where the function changes its sign. The interval containing the root needs to be identified to begin the search. An interval based on the admissible region for our problem is chosen. A root lies in the interval (a, b) if $f(a)$ and $f(b)$ have opposite signs. The function is evaluated at the interval's midpoint and its sign is examined. The midpoint is used to replace whichever limit has the same sign. After each iteration, the bounds containing the root decrease by a factor of two. If after n iterations, the root is known to be within an interval of size ϵ, then after the next iteration it will be within an interval of size $\epsilon/2$. The iterations are carried out until the function value is below tolerance. Figure 5. illustrates two points on the function, which constitute the boundary of an interval that contains a root. This interval can also be called a bracket. Figure 6. shows another situation encountered while root finding.

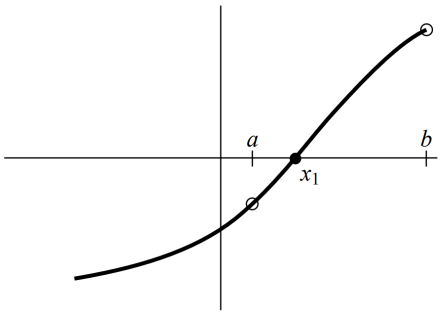

Figure 5. An isolated root x_1 bracketed by two points a and b at which the function has opposite signs.

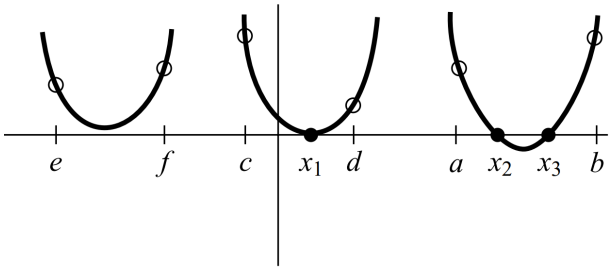

Figure 6. There is not necessarily a sign change in the function near a double root (in fact, there is not necessarily a root!)

An example of a function plot was made for $(\rho_{2hyp} - \rho_2)$ for an initial hypothesis (ρ_1, ρ_2) in case of three revolutions and AMR 10 (m^2/kg). Here ρ_{2hyp} is the value of range hypothesis at second epoch entering the shooting method from OBVIOD. The plot is shown in Figure 7 below. The function is continuous with multiple roots, the bisection method could be used for this type of function. Since the function has multiple roots, it will need to be divided into various intervals (also called brackets) in order for the Bisection method to find all the roots in the desired intervals.

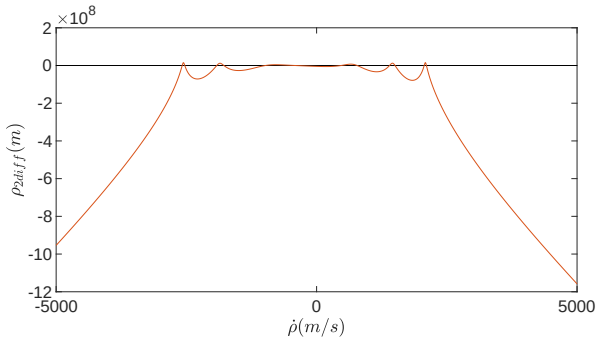

Figure 7. Function plot made by varying $\dot{\rho}$ values for a given ρ_1, ρ_2. Here ρ_{2diff} refers to the difference between ρ_{2hyp} entering shooting from OBVIOD and the instantaneous ρ_2 inside shooting IOD.

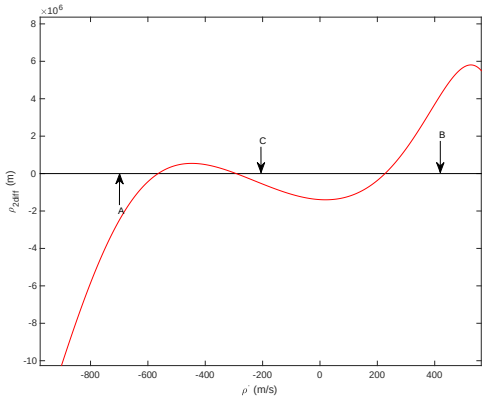

Figure 8. Function bounds resulting from semi major axis constraints.

2.2.1. Constraints for Brackets in Bisection method

Brackets are searched in the admissible region defined by the semi major axis, between 41,000 km and 43,000 km. The orbital velocity expression from the vis-viva equation is:

$$v^2 = \frac{GM}{((\frac{2}{r}) - (\frac{1}{a}))} \tag{11}$$

If the maximum semi major axis value (43,000 km) is substituted in the above quadratic equation, one gets two roots for the velocity. The ρ, $\dot{\rho}$ satisfy the geocentric position and velocity as following:

$$r(\rho) = \overrightarrow{r_s} + \rho\overrightarrow{u} \tag{12}$$

$$v(\rho, \dot{\rho}) = \overrightarrow{v_s} + \rho\dot{\overrightarrow{u}} + \dot{\rho}\overrightarrow{u} \tag{13}$$

The information about r_s and v_s (station position and velocity) is available. u (line of sight angle) and $\dot{u}$ are computed from the angular positions and velocities. The only unknown in equation (10), $\dot{\rho}$ can be computed using velocity values one gets from the constraints. Using the values from the semi major axis constraints, one obtains a quadratic in range-rate. Rearranging equation (11) and using (12) and (13) one gets

$$a = \frac{rGM}{2GM - r(\dot{\rho}\overrightarrow{u} + \rho\dot{\overrightarrow{u}} + \overrightarrow{v_s})^2} \tag{14}$$

The roots of this quadratic will correspond to the bounds of our function by inserting respective a values. For the minimum value only one value of $\dot{\rho}$ is obtained whereas inserting the maximum value results in two values of $\dot{\rho}$. These $\dot{\rho}$ values are used as the starting brackets for the bisection method. Point C in the Figure 8. corresponds to the semi major axis minimum on the $\dot{\rho}$ axis and points (A, B) correspond to the maximum. Intervals containing multiple roots are separated into smaller brackets. The Lambert's problem has multiple possible solutions for one or more number of revolutions. These solutions are (2m + 1) in number, where m is the number of revolutions. For each number of revolutions higher than zero, there are two solutions. They are called as long-path and short-path orbits. For the same value of semi-major axis, the long-path orbit will have a higher eccentricity than the short- path orbit. [8] gives more information about the multiple-revolution Lambert's problem.

Similarly eccentricity can be expressed using the geocentric position, velocity and semi major axis as:

$$e = \sqrt{1 - \frac{(\overrightarrow{r} \times \overrightarrow{v})^2}{\mu a}} \tag{15}$$

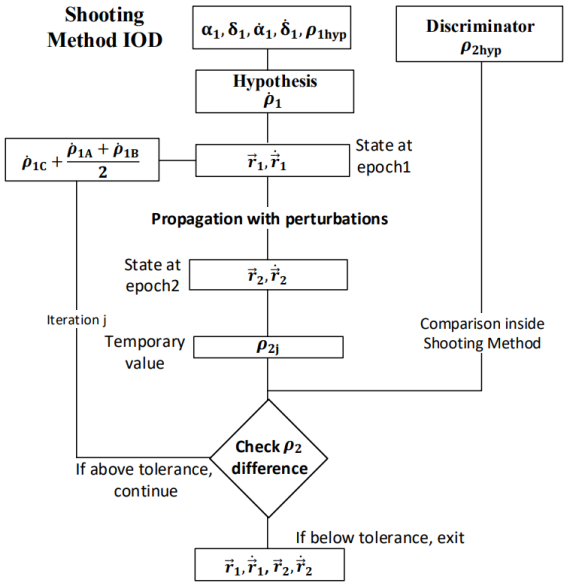

Figure 9. Schematic of shooting IOD with bisection.

Once one substitutes the value of a from equation (11) and values of $\overrightarrow{r}$ and $\overrightarrow{v}$ in terms of ρ, $\dot{\rho}$, one obtains a quartic equation in $\dot{\rho}$. The solution to the quartic equation was comparatively difficult to calculate, contrary to the semi major axis relation. Hence, only the latter was used to define function bounds. The equation (12) also shows that for every value of semi major axis we will have two values of eccentricity, with only one exception of minimum value of semi major axis. [8] discusses various constraints that can be possibly used to reduce the number of practical solutions to be computed from a Multiple-Revolution Lambert's Problem. These constraints were investigated, but the ranges of semi major axis originating from them were found to be a subset of the constraints defined in the beginning of this subsection. However, the constraints described in [8] are more generic and could be tailored for cases where the user could define the apogee, perigee limits for a specific mission and find the solutions for a given orbital problem. The authors also mention about the relationship between eccentricity and semi major axis, interested readers could refer to their paper for more details.

2.3. Functioning in Bisection

Once the brackets containing the roots are found, each bracket is followed one by one starting from the positive value of $\dot{\rho}$ corresponding to the a_{max} root. The resulting schematic of the Shooting IOD with the Bisection method is shown in Figure 9.

The ρ_1, ρ_2 hypothesis enters the Shooting IOD. The $\dot{\rho}$ brackets containing roots are computed using the semi major axis admissible region. The brackets are followed one by one. $\alpha_1, \delta_1, \dot{\alpha}_1, \dot{\delta}_1, \rho_1, \dot{\rho}_1$ along with $\dot{\rho}_1$ hypothesis are used to compute an orbit. It is propagated to the second epoch using perturbations. The resulting ρ_2 is compared by the ρ_{2hyp} that entered the Shooting IOD. The $\dot{\rho}_1$ root is computed such that the difference between the computed ρ_2 and the ρ_{2hyp} is below a certain threshold.

The $\dot{\rho}_1$ root depends on the ρ_1 value which changes through different iterations. Hence the size of the brackets changes as well. The strategy adopted in case the a bracket containing root disappears, is to take the root from the adjacent bracket (the one which was not searched before).

The values of α_2 and δ_2 are not used in the Shooting IOD. These values could be used along with ρ_2 by exploiting the Pythagorean theorem. However, the resulting differences in state at the second epoch would be positive or null. Since the strategy in Bisection method works by detecting the change in sign of the functions, this was not possible. Consequently, only the difference between ρ_2 and ρ_{2hyp} was used. The values of α_2 and δ_2 are used in the final discriminator of Shooting-OBVIOD. The structure of the latter is given in the previous section.

2.3.1. Use of brackets inside Shooting-OBVIOD

An interval containing root in constrained region is termed as a bracket. As already stated, the $\dot{\rho}_1$ root depends on the ρ_1 value which may change during different iterations. Hence the size and number of brackets change as well. The brackets are always searched one by one starting from one of the two values of $\dot{\rho}$ corresponding to the semi major maximum. The numbering of brackets starts from the first interval containing root between $\dot{\rho}_{amin}$ and $\dot{\rho}_{amax}$ (positive value). The description of brackets originating from the admissible region is shown in Figure 10. for a given object and (ρ_1, ρ_2).

In the original OBVIOD algorithm, the number of possible solutions could go up to six for a case of three revolutions. The admissible region used in bisection method and the definition of brackets reduces the number of possible solutions to be computed. This is essential when the numerical propagation is expensive in terms of time especially in multi-revolution scenarios.

In case the bracket being followed disappears because there is no root in that interval anymore for a (ρ_1, ρ_2), the root is searched in the next bracket. This is achieved by awarding a serial number to the brackets. For example in situations where the first bracket is being followed but the corresponding root disappears, the next bracket is awarded as serial number 1 and is searched for the root. An example of number of brackets reducing from one rho pair to another is shown in Figure 10. The number of roots in the admissible region reduces from two to one.

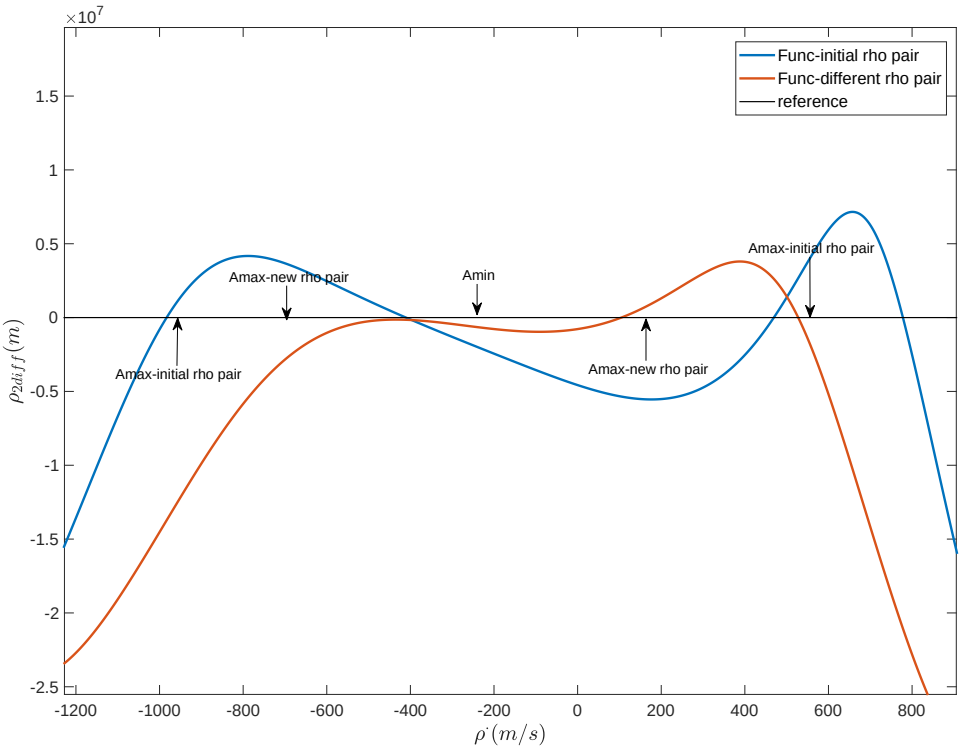

Figure 10. Function plots showing change in number of roots with different ρ_1, ρ_2.

2.3.2. The working of Bisection-Shooting in OBVIOD

In the present version of the algorithm with Bisection-Shooting for IOD, the same hypothesis variables (ρ_1, ρ_2) are used as from original OBVIOD. This pair of variables provides the advantage of a more favorable search space than $\rho_1, \dot{\rho}_1$. Once the range hypothesis is made, this pair enters the Shooting scheme where the $\dot{\rho}$ hypothesis is made in order to determine the orbit for a given rho pair. This orbit determination includes a propagation step with perturbations. Once the initial orbit is determined, the Mahalanobis distance is computed using $(\alpha_2, \delta_2, \dot{\alpha}_2, \dot{\delta}_2)$ as the discriminator inside the BFGS algorithm. This discriminator makes the Shooting-OBVIOD algorithm similar to the initial value orbit determination algorithm. However, due to the change of iteration variables from $\rho_1, \dot{\rho}_1$ (initial value algorithm) to ρ_1, ρ_2 in BFGS, the function topography is kept optimal. The variable ρ_2 is used only for the search in the BFGS algorithm.

3. TESTS AND RESULTS

3.1. Simulation of input files

The adopted GEO survey strategy consists of repeatedly scanning a declination stripe with a fixed right ascension. The declination interval is chosen as ±8° for each right ascension. Observations were simulated using the Zimmerwald station coordinates to get topocentric angular positions over the length of 2 to 3 minutes. The TLEs used were extracted from Spacetrack objects catalog. Perturbations were added for: geopotential terms (upto second degree and order), solar radiation pressure, third body attraction forces for Sun and Moon. In the following tests observations simulated for the GEO regime were considered. The constraints applied on different elements were: inclination $< 10°$, eccentricity < 0.3, semimajor axis between 41,000 km and 43,000 km. Two tracklets are tested at a time. They are separated by a few hours, one or two revolutions.

3.2. Comparison between unperturbed OBVIOD and Bisection Shooting

Both the methods are compared by varying the number of revolutions and AMR values. All the tests are done with different objects so as to increase the sample size. The number of tracklet pairs tested are still limited owing to the high computation time consumed by the numerical propagator used in Shooting-OBVIOD.

Nevertheless, variation of AMR values while keeping the number of revolutions constant and vice-versa does give an insight about the limitations of unperturbed OBVIOD and how well Shooting- OBVIOD is able to overcome them. The results are shown starting from Figure 11. to

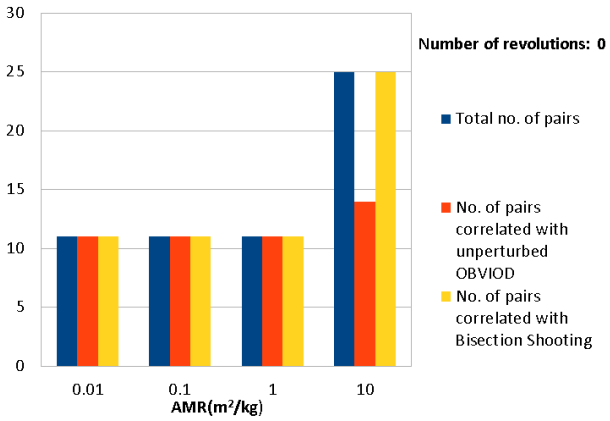

Figure 11. For tracklet pairs separated by less than 1 revolution, the unperturbed OBVIOD performs equally well except in case of very high AMR.

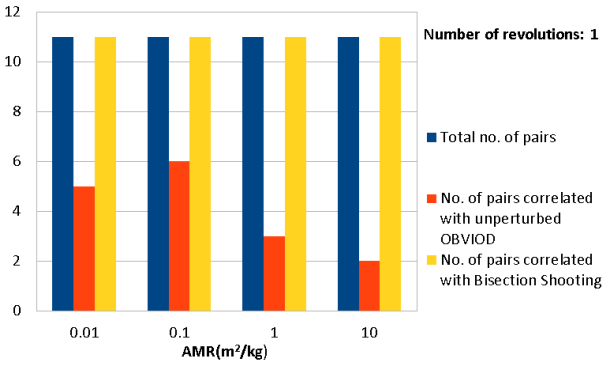

Figure 12. The performance of the unperturbed OBVIOD begins to worsen starting from a case of tracklets separated by 1 revolution.

Figure 18. The degradation of unperturbed OBVIOD results is evident for 1 or more revolutions and similarly for very high-area-to-mass-ratio (HAMR) objects. This is expected because with increase in AMR and tof the perturbations have a higher impact, especially the solar radiation pressure.

4. CONCLUSIONS

Unperturbed OBVIOD begins to fail with increase in number of revolutions. This also happens for a high-area-to-mass ratio object. The proposed algorithm performs well even in case of HAMR values and multiple revolutions when compared to the unperturbed OBVIOD. Shooting OBVIOD could replace the latter in case correlation doesn't take place.

However, the Shooting-OBVIOD comes with some challenges. It works on the basis of brackets which can disappear later in the iterations. In such cases, one could miss the solution (no correlation) because the bracket containing root was not one of the available brackets. There are

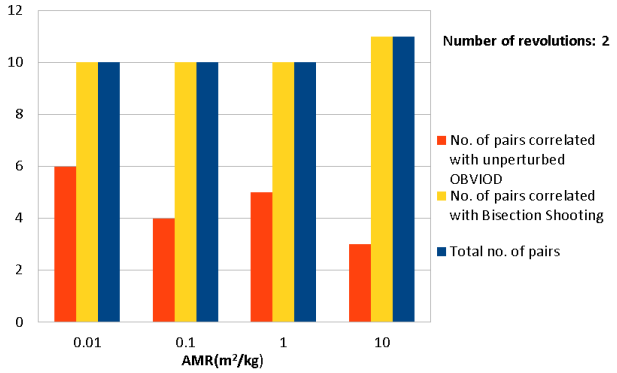

Figure 13. The performance of unperturbed OBVIOD fluctuates between 1 and 2 revolutions, with highest AMR value resulting in minimum number of correlations.

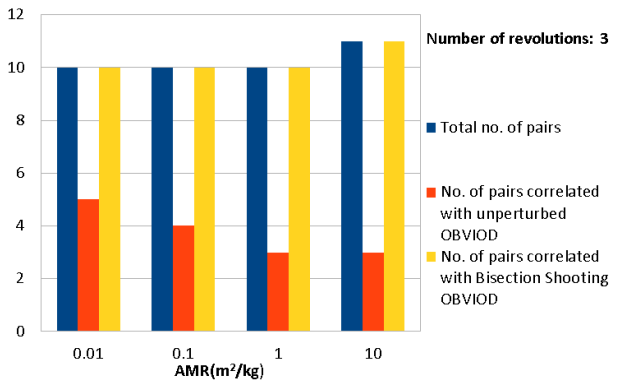

Figure 14. This case shows a clear decline of number of correlations with the increase in AMR value.

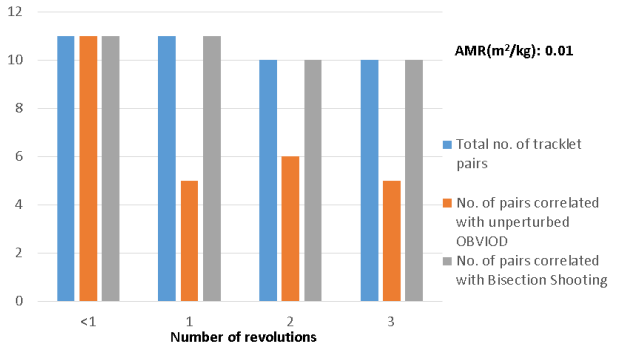

Figure 15. For a small AMR value, the no. of correlations decrease with increase in number of revolutions however, one still gets around 50% of the tracklet pairs correlated.

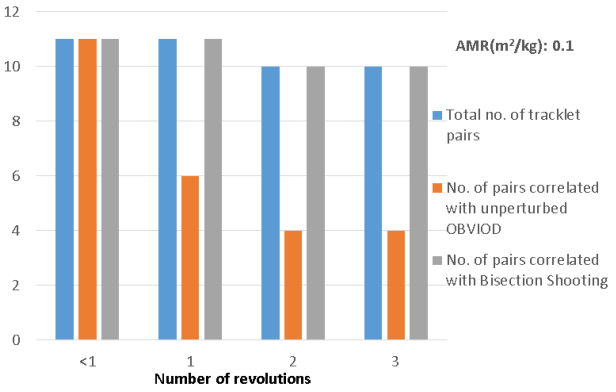

Figure 16. For a slightly higher AMR, the decline in number of correlations is evident with increasing number of revolutions.

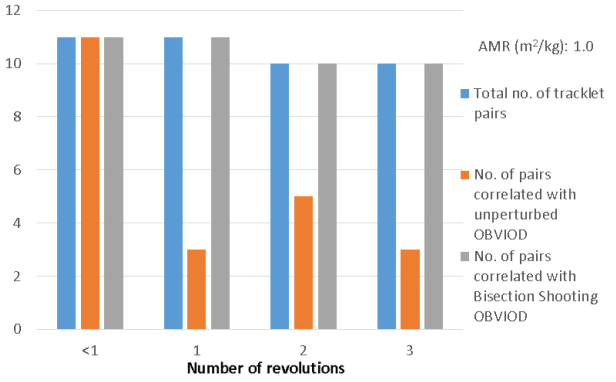

Figure 17. The number of correlations further decreases with increase in the AMR value. Although, the performance does fluctuate between different number of revolutions.

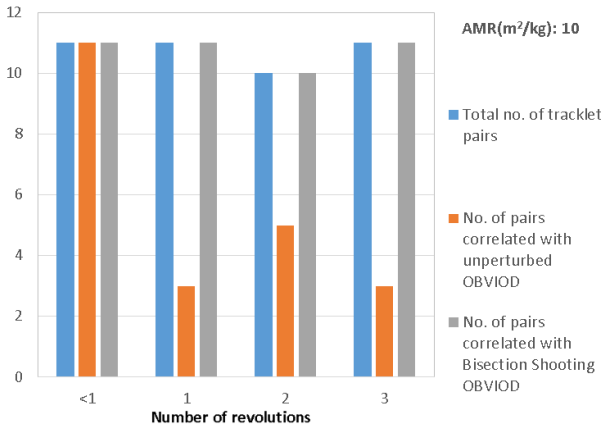

Figure 18. The performance for very HAMR value is comparable to the previous case, when effect of number of revolutions is considered.

cases where none of the brackets resulting from the initial hypothesis contain the root. The right bracket may or may not appear in the later iterations. This method has a dependency on the initial rho pair hypothesis that is taken to begin the iterations. Besides, the numerical propagation makes this algorithm much more slower when compared to the unperturbed OBVIOD.

ACKNOWLEDGMENTS

The authors would like to extend gratitude towards the Swiss National Science Foundation for funding this research and the University of Bern for providing various facilities.

REFERENCES

1. Harleen K. Mann, Dr. Alessandro Vananti, Prof. Thomas Schildknecht, (2020). Shooting Method to allow for perturbations in the Optimized Boundary Value Initial Orbit Determination, 71^{st} International Astronautical Congress (IAC) - The CyberSpace Edition, IAC-20-A6-9-x57579
2. T. Schildknecht, (2007).Optical surveys for space debris *Astronomy and Astrophysics Review*, 47-50
3. J.A. Siminski, H. Fiedler, T. Schildknecht, (2013). Track Association Performance of the Best Hypothesis Search Method, 6th European Conference on Space Debris, Darmstadt, Germany, 22-25.
4. J.A. Siminski, O. Montenbruck, H. Fiedler, T. Schildknecht, (2014). Short-arc tracklet association for geostationary objects, *Advances in Space Research* 53, 1184-1194.
5. W.H. Press, S.A. Teukolsky, W.T. Vetterling, B.P. Flannery,*Numerical Recipes in Fortran 77*, Cambridge University Press, second ed.,1992.
6. P.C. Mahalanobis, (1936). On the generalised distance in statistics*Proceedings of the National Institute of Sciences of India*, 2 (1): 49–55.
7. Dario Izzo, (2015). Revisiting Lambert's problem, *Celestial Mechanics and Dynamical Astronomy* Quantities, 121:1–15
8. Gang Zhang and Daniele Mortari and Di Zhou, 2010, Association of optical tracklets from a geosynchronous belt survey via the direct Bayesian admissible region approach, *Journal of Guidance, Control and Dynamics*, 33 (6):1779–1786
9. A. Milani, G.F. Gronchi, M.D.M Vitturi, Z. Knezevic, (2004). Orbit Determination with Very Short Arcs. I Admissible Regions , *Celestial Mech. Dyn. Astron. 90* (1–2), 57–85.